Achieving Porous Carbon Fibers Pretreated With a Swarm of CO2 Micro-Nanobubbles

Joon Hyuk Lee
Hanyang University - Seoul Campus: Hanyang University
Soon Hong Lee
Anyang University
Dong Hack Suh (dhsuh@hanyang.ac.kr)
Hanyang University - Seoul Campus: Hanyang University https://orcid.org/0000-0003-0485-7557

Research Article

Keywords: Carbon dioxide utilization, Carbon fiber, Petroleum pitch, Micro-nanobubbles, Surface characteristics, Green chemistry

Posted Date: February 25th, 2021

DOI: https://doi.org/10.21203/rs.3.rs-221148/v1

Abstract

Using petroleum pitch is touted as a sustainable method to fabricate carbon fibers, yet requires further advances in inevitable pore decrease after post-treatment. In an effort to circumvent this upper limit, renewable resources are widely used in the production of commercial carbon fibers. Here we show that dissolved micro-nanobubbles of CO_2 in pretreatment may aid in the pore-growth of carbon fibers during activation. The results confirm that micro-nanobubbles increase specific surface (39.21 %) and micropore (16.44 %) areas of a sample. The chemical state of the elements revealed that there were no marked impurities. The observed behaviors can be understood by the following; 1) Partial O atoms released from dissolved micro-nanobubbles may attach to surrounding CO during activation, thereafter results in a higher mass of CO_2. 2) Partial O atoms may directly interact with C from unmatured crystallites and form additional CO. We further denote optimized conditions based on the derived mechanism. This study provides a new strategy for the development of highly surface carbonaceous materials, thus possibly stimulating more research on advanced performance adsorbents or electrode materials.

Introduction

Carbon materials are of fundamental importance and developing their applications have broad implications in energy, electronics, and environment (Liu et al. 2019; Gopinath et al. 2020). Currently, the most commonly used carbon materials include graphene, activated carbons, and carbon fibers (Qu et al. 2020; Blankenship et al. 2017; Zhou et al. 2019; Yoda et al. 2019). Carbon fibers possess the interest aroused in ease of handling and mechanical flexibility compared to powdered or granular carbon materials. In the last decades, there was increasing attention to an eco-sustainable development of carbon fibers based on non-renewable fossil fuels. Amongst the possible candidates for precursors, petroleum pitch as a residue of the petrochemical industry has been widely proposed (Guo et al. 2020; Liu et al. 2020; Ning et al. 2020). We further abbreviate petroleum pitch as pitch for convenience. Pitch is functionalized of aromatic hydrocarbons with mesophase feature (Zhang et al. 2019). These sp^2-C dominant molecules are responsible for the extensive interconnection during stabilization (oxidation), carbonization, and activation. After activation, surface modification using various chemicals has become a crucial necessitate to expand their applications (Wang et al. 2019; Goswami et al. 2017; Yu et al. 2017; Lee et al. 2020). From most reports, however, there is an inevitable decrease in surface characteristics after post-treatment due to pore-blocking or introduced surface functional moieties (Fig. 1). Despite the impressive progress, surface characteristics of pitch-based carbon fibers are far from satisfying compared to advanced carbon materials. To this aim, the idea of achieving high surface characteristics during activation to endure the decrease in post-treatment has been industrialized. Using CO_2 as an activation agent seems viable in most methodology-driven works, since it is facile to control, abundant, and recyclable (Zhang et al. 2020). CO_2 capture and utilization techniques are recognized as sensible resource management for sustainable development (Zhou et al. 2020; Liu et al. 2015; Osman et al. 2020; Arun et al. 2020; Ochedi et al. 2020). Xing and coworkers have hinted that the hole-making function could be further transverse to the hole-enlarging function during CO_2 activation under high temperature (Lan et

al. 2019). The findings of Jaroniec and coworkers are at odds with the claims of Xing and coworkers that CO_2 activation noted more considerable structure development than KOH activation under high temperature (Choma et al. 2016). To date, the vast majority of CO_2 utilization for achieving high surface characteristics is performed during activation.

Here, we present a novel method for fabricating carbon fibers with the aid of CO_2 micro-nanobubbles in pretreatment. Micro-nanobubbles are gas bubbles reported to have diameters on the order of micro and nanometers. Conceivably, early introduced gas bubbles may move upward by buoyancy and gradually dissolve on immersed substrates. Their existence seems paradoxical due to the large Laplace pressure inside these spherical-cap-shaped objects. Although widely used, critical commentaries have described the questionable existence of gas bubbles for decades and named as the classic Laplace pressure bubble catastrophe theory (Alheshibri et al. 2016; Lohse et al. 2015). A series of work has recently shown that tiny particles could be detected via particle tracking or scattering in transparent water. Some scholars believe that these detected particles are mainly gas bubbles, while others classify them as solid impurities (Yasui et al. 2018; Jadhav et al. 2020). Since it may beyond the scope of this letter to end the lasting debate, we gently reconcile the history of micro-nanobubbles with carbonaceous materials. Several generating strategies of gas bubbles currently exist due to the maturity of gas bubble generation techniques (Haris et al. 2020). In this work, the mechanical agitation method was adopted to generate micro-nanobubbles. The as-prepared carbon fiber exhibits hierarchically interconnected micro- and macropores with high surface characteristics. By accounting for the time-dependent feedback during fabrication, we find that the introduction of micro-nanobubbles in pretreatment and contact time of CO_2 gas in activation is consistent with the pore growth. Combined with elemental analysis, surface characteristics also quantifies the amount of chemical deposit and verifies that none of the major impurities were found in all cases. This opens a viable hypothesis of the existence of gas bubbles that provides an impetus for future environmental chemistry research.

Experimental

Materials

Fig. 2 shows a schematic of the fabrication method of samples. Pitch with a softening point of 300 °C was used as a precursor (see S1 for details). Melt-spinning was conducted via spinning nozzle equipment at 300 °C. A spinneret has designed with a ratio of L D^{-1} = 2 (length: 0.6 mm, diameter: 0.3 mm). A fiber shape of the resultant was suitable for stabilization, carbonization, and activation. Before stabilization, micro-nanobubbles were introduced to the sample using a CO_2 micro-nanobubble generator for 3 hr. A generator with 40 mm and 130 mm in diameter and height, respectively, of twin protruding bubble refiners were employed for micro-nanobubble generation. The flow of CO_2 was fixed at 0.2 mL min^{-1} with an ambient room temperature. A sample without micro-nanobubbles was also prepared as a counterpart. Stabilization was held in air mood (2 L min^{-1}) of 290 °C for 3 hr. The stabilized samples were subsequently carbonized under N_2 gas (2 L min^{-1}) and heated to 880 °C (see S2 for the optimized

temperature). Once the temperature has reached the suggested temperature, activation was done by adding CO_2 gas instead of N_2 gas for 3 hr and 6 hr, respectively. The resultant samples were denoted as ACF-H and BACF-H. B refers to micro-nanobubbles and H is the activation time (hr).

Methodology

Surface characteristics of the obtained samples were determined by Brunauer-Emmett-Teller (BET) and Barrett-Joyner-Halenda (BJH) methods (ASAP 2460, Micrometrics). Pore size distributions were derived from N_2 adsorption measurements. Prior to the physisorption analysis, samples were heated at 300 °C for 12 hr with a vacuum state of 1.33×10^{-3} Pa (VacPrep 061, Micromeritics). Morphologies were analyzed using field emission scanning electron microscopy (Carl Zeiss, SIGMA) after gold sputter coating of samples for 60 s. An operating acceleration voltage was 2.00 kV. Chemical ratios were examined through X-ray photoelectron spectroscopy (AXIS NOVA, KRATOS) and energy-dispersive X-rey spectrometer (S-4300, Hitachi).

Results And Discussion

Surface characteristics

To investigate the possible structural changes due to pretreatment and activation using various forms of CO_2, the textural properties of samples are studied (see S3 for tabulated values). Micro-nanobubble-pretreated samples have typically exhibited fascinating BET specific surface areas as plotted in Fig. 3(a). The BET specific surface area was 1209 $m^2\ g^{-1}$ after pretreatment and 3 hr of CO_2 activation, which is 39.21 % higher than the surface area of ACF-3 (735 $m^2\ g^{-1}$). Likewise, BACF-3 showed a 16.44 % increase in micropores when compared with the bare support (Fig. 3(b)). As the activation time using CO_2 increases from 3 hr to 6 hr, the BET specific area of ACF-3 and BACF-3 increased 7.20 % and 13.33 %, respectively. CO_2 is acknowledged as the most stable form of oxidized carbon compounds. Nevertheless, it reacts easily to form additional C-C and/or C-H bonds under a high-energy input. Given that, the use of various CO_2 forms in both pretreatment and activation may lead to the highest surface characteristics (Fig. 3(d)). As observed in the yield curve (Fig. 3(a)), all samples showed the loss of their total mass due to the decomposition of unmatured polymers via a sandwich of CO_2 treatment (Yoda et al. 2018). Although BACFs possessed higher surface characteristics than ACFs, the yield curves were 10.92 % and 11.52 % lower in 3 hr and 6 hr, respectively. The upward peaks in N_2 adsorption-desorption isotherms suggest that all samples are of Type I, which is typical for microporous materials (Fig. 3(c)). The broadening of peaks shows an increasing adsorption trend and does not flatten at P/P^0 between 0.8 ~ 1.0, which verifies the multilayer adsorption. Alongside the typically characterized adsorption force in microporous materials, the van der Waals force is given on the adsorption potential within micropores. This indicates that all samples have a large micropore region and a comparably small mesopore region. N_2 volume adsorption-desorption isotherms are also in good agreement with the inert graph in Fig. 3(b).

The chemical state of elements

Introduction of micro-nanobubbles and post-treatment of CO_2 (6 hr) seems to be the key factors to achieve superior surface characteristics. However, there are underlying uncertainties whether the samples are free of any impurities. Acknowledging that impurities are more likely to be attached to the samples with high BET specific surface, ACF-6 and BACF-6 were chosen to observe the chemical state of elements. Both samples reveal porous characteristics with no visible impurities (Figs. 4(a)-(b)). According to the average chemical proportion, C and O are considered to be major elements present in both samples (Fig. 4(c) and S4). The amount of C and O was 2.91 % and 2.93 % higher in ACF-6 and BACF-6, respectively. Evidently, C and O ratio difference is mainly due to the side chains of partial oxygen-containing functional groups (C-O, O-C=O, and C-C) introduced on the surface. Only N can be distinguished in the category of minor components (ACF-6: 1.65 % and BACF-6: 1.63 %). This is attributed to residual nitrogen from pitch. The wide scan spectrum displayed photoelectron lines in the order of C1s (approx. 288 eV) > O1s (530 eV) > N1s (400 eV). No characteristic peaks of any impurities were noticed, suggesting that micro-nanobubbles are solely the major culprit of high surface characteristics.

We merely hypothesized that dissolved micro-nanobubbles at the frontline of stabilization may chemically react with the surface and aid for pore-growth (Fig. 2(b)). However, it is still an arduous quest to theoretically understand the microchemical behavior of dissolved micro-nanobubbles without satisfactory reasons. Inspired by the two scenarios proposed with CO_2 activation, we track O atoms under the inclusion of surrounding elements (Figs. 4(d)-(e)). On the one hand, dissolved micro-nanobubbles may release partial O atoms attached to the surface as the temperature increases. Partial O atoms could form additional CO_2 with surrounding CO during activation, resulting in a higher mass of CO_2 activation (Nabais et al. 2008). Another interesting approach lies on the partial O atoms, which are not attached with surrounding CO. Partial O atoms may directly compromise with C of crystallites and result in additional CO. The activation reaction could be promoted while the unmatured carbonaceous fiber consumes CO, which results in additional pore-growth (Lan et al. 2019). In summarization, dissolved micro-nanobubbles may not generate pores by themselves, but rather act as a swarm of catalyst at the beginning of stabilization. These chemical interactions made our samples bear great application potential in high-performance adsorbents or electrode materials.

Conclusion

A novel sandwich technique of CO_2 in pretreatment and activation has been explored for achieving high surface characteristics. BET and BJH analyses determine that the introduction of micro-nanobubbles in pretreatment was 29.89 % more effective for increasing BET specific surface compared with CO_2 gas variation from 3 hr to 6 hr in activation. SEM images indicate the formation of porous surface in the order of BACF-6 > ACF-6. The estimated chemical elements were mainly C, O, and N in all samples, whereas there were no significant impurities. Partial O atoms from the dissolved micro-nanobubbles are believed to be the catalytic driving force for surface modification. On the basis of its facile and green fabrication

process without the requirement of additional chemicals, great versatility in relevant fields is expected. It further lays the groundwork for utilizing CO_2 to improve the interatomic potentials of carbonaceous materials. While this letter acts as an introduction of micro-nanobubbles for the synthesis of carbonaceous materials during pretreatment, we will experimentally track partial O atoms in forthcoming work.

Abbreviations

ACF Activated carbon fiber

C Carbon

CO Carbon monoxide

CO_2 Carbon dioxide

N Nitrogen

O Oxygen

Declarations

Funding

This research did not receive any specific grant from funding agencies in the public, commercial, or non-for-profit sectors.

Conflict of interest

The authors declared no conflicts of interest.

Ethics approval

Not applicable

Consent to participate

Not applicable

Consent for publication

Not applicable

Availability of data and material

The data that support the findings of this study are available from the corresponding author, upon reasonable request.

Code availability

Not applicable

Author's contributions (CRediT)

Conceptualization: Joon Hyuk Lee & Dong Hack Suh, Methodology: Soon Hong Lee & Dong Hack Suh, Writing – original draft preparation: Joon Hyuk Lee, Writing – review and editing: Soon Hong Lee & Dong Hack Suh, Visualization – Joon Hyuk Lee.

References

1. Arun J, Gopinath KP, Sivaramakrishnan R, SundarRajan P, Malolan R, Pugazhendhi A (2020) Technical insights into the production of green fuel from CO2 sequestered algal biomass: A conceptual review on green energy. Sci Total Environ 142636. https://doi.org/10.1016/j.scitotenv.2020.142636
2. Alheshibri M, Qian J, Jehannin M, Craig VS (2016) A history of nanobubbles. Langmuir 32(43):11086-11100. https://doi.org/10.1021/acs.langmuir.6b02489
3. Blankenship II TS, Balahmar N, Mokaya R (2017) Oxygen-rich microporous carbons with exceptional hydrogen storage capacity. Nat Commun 8:1545. https://doi.org/10.1038/s41467-017-01633-x
4. Choma J, Osuchowski L, Marszewski M, Dziura A, Jaroniec M (2016) Developing microporosity in Kevlar®-derived carbon fibers by CO2 activation for CO2 adsorption. J CO2 Util 16:17-22. https://doi.org/10.1016/j.jcou.2016.05.004
5. Gopinath KP, Vo DVN, Prakash DG, Joseph AA, Viswanathan S, Arun J (2020) Environmental applications of carbon-based materials: a review. Environ Chem Lett 1-26. https://doi.org/10.1007/s10311-020-01084-9
6. Goswami M, Phukan P (2017) Enhanced adsorption of cationic dyes using sulfonic acid modified activated carbon. J Environ Chem Eng 5(4):3508-3517. https://doi.org/10.1016/j.jece.2017.07.016
7. Guo J, Li X, Xu H, Zhu H, Li B, Westwood A (2020) Molecular Structure Control in Mesophase Pitch via Co-Carbonization of Coal Tar Pitch and Petroleum Pitch for Production of Carbon Fibers with Both High Mechanical Properties and Thermal Conductivity. Energy Fuels 34(5):6474-6482. https://doi.org/10.1021/acs.energyfuels.0c00196
8. Haris S, Qiu X, Klammler H, Mohamed MM (2020) The use of micro-nano bubbles in groundwater remediation: A comprehensive review. Groundw Sustain Dev 100463. https://doi.org/10.1016/j.gsd.2020.100463
9. Jadhav AJ, Barigou M (2020) Bulk Nanobubbles or Not Nanobubbles: That is the Question. Langmuir 36(7): 1699-1708. https://doi.org/10.1021/acs.langmuir.9b03532

10. Lan X, Jiang X, Song Y, Jing X, Xing X (2019) The effect of activation temperature on structure and properties of blue coke-based activated carbon by CO2 activation. Green Process Synth 8(1):837-845. https://doi.org/10.1515/gps-2019-0054
11. Lee JH, Lee SH, Suh DH (2020) CO 2 treatment of carbon fibers improves adsorption of fuel cell platinum. Environ Chem Lett 1-6. https://doi.org/10.1007/s10311-020-01105-7
12. Liu D, Li C, Wu J, Liu Y (2019) Novel carbon-based sorbents for elemental mercury removal from gas streams: A review. Chem Eng J 123514. https://doi.org/10.1016/j.cej.2019.123514
13. Liu J, Chen X, Xie Q, Liang D (2020) Controllable synthesis of isotropic pitch precursor for general purpose carbon fiber using waste ethylene tar via bromination–dehydrobromination. J Clean Prod 271: 122498. https://doi.org/10.1016/j.jclepro.2020.122498
14. Liu Q, Wu L, Jackstell R, Beller M (2015) Using carbon dioxide as a building block in organic synthesis. Nat Commun 6:5933. https://doi.org/10.1038/ncomms6933
15. Lohse D, Zhang X (2015) Surface nanobubbles and nanodroplets. Rev Mod Phys 87(3):981. https://doi.org/10.1103/RevModPhys.87.981
16. Nabais JV, Carrott P, Carrott MR, Luz V, Ortiz AL (2008) Influence of preparation conditions in the textural and chemical properties of activated carbons from a novel biomass precursor: The coffee endocarp. Bioresour Technol 99(15):7224-7231. https://doi.org/10.1016/j.biortech.2007.12.068
17. Ning H, Guo D, Wang X, Tan Z, Wang W, Yang Z, Wu M (2020) Efficient CO2 electroreduction over N-doped hieratically porous carbon derived from petroleum pitch. J Energy Chem 56:113-120. https://doi.org/10.1016/j.jechem.2020.07.049
18. Ochedi FO, Liu D, Yu J, Hussain A, Liu Y (2020) Photocatalytic, electrocatalytic and photoelectrocatalytic conversion of carbon dioxide: a review. Environ Chem Lett 1-27. https://doi.org/10.1007/s10311-020-01131-5
19. Osman AI, Hefny M, Maksoud MA, Elgarahy AM, Rooney DW (2020) Recent advances in carbon capture storage and utilisation technologies: a review. Environ Chem Lett 1-53. https://doi.org/10.1007/s10311-020-01133-3
20. Qu ZB, Feng WJ, Wang Y, Romanenko F, Kotov NA (2020) Diverse nanoassemblies of graphene quantum dots and their mineralogical counterparts. Angew Chem 132(22):8620-8629. https://doi.org/10.1002/ange.201908216
21. Wang Z, Jin H, Wang K, Xie Y, Ning J, Tu Y, Zeng H (2019) A two-step method for the integrated removal of HCl, SO2 and NO at low temperature using viscose-based activated carbon fibers modified by nitric acid. Fuel 239:272-281. https://doi.org/10.1016/j.fuel.2018.11.002
22. Yasui K, Tuziuti T, Kanematsu W (2018) Mysteries of bulk nanobubbles (ultrafine bubbles); stability and radical formation. Ultrason Sonochem 48:259-266. https://doi.org/10.1016/j.ultsonch.2018.05.038
23. Yoda T, Shibuya K, Myoubudani H (2018) Preparation of activated carbon fibers from mixtures of cotton and polyester fibers. Measurement 125:572-576. https://doi.org/10.1016/j.measurement.2018.05.044

24. Yoda T, Shibuya K, Myoubudani H (2019) Preparation and adsorption performance evaluation of activated carbon fibers derived from rayon. SN Appl Sci 1(9):1-7. https://doi.org/10.1007/s42452-019-1061-8
25. Yu Y, Zhang C, Yang L, Chen JP (2017) Cerium oxide modified activated carbon as an efficient and effective adsorbent for rapid uptake of arsenate and arsenite: Material development and study of performance and mechanisms. Chem Eng J 315:630-638. https://doi.org/10.1016/j.cej.2016.09.068
26. Zhang C, Li Y, Li Y, Zhang W, Wang X, He X, Yu M (2019) Synthesis and Zn (II) modification of hierarchical porous carbon materials from petroleum pitch for effective adsorption of organic dyes. Chemosphere 216:379-386. https://doi.org/10.1016/j.chemosphere.2018.10.164
27. Zhang N, Pan Z, Zhang Z, Zhang W, Zhang L, Baena-Moreno FM, Lichtfouse E (2020) CO2 capture from coalbed methane using membranes: a review. Environ Chem Lett 18:79–96. https://doi.org/10.1007/s10311-019-00919-4
28. Zhou D, Yu M, Fan Y, Wang Z, Dang G, Zhang Q, Xie J (2020) Sodium-induced solid-phase hydrogenation of carbon dioxide to formate by mechanochemistry. Environ Chem Lett 1-5. https://doi.org/10.1007/s10311-020-00974-2
29. Zhou Z, Liu T, Khan AU, Liu G (2019) Block copolymer–based porous carbon fibers. Sci Adv 5(2): eaau6852. https://doi.org/10.1126/sciadv.aau6852

Figures

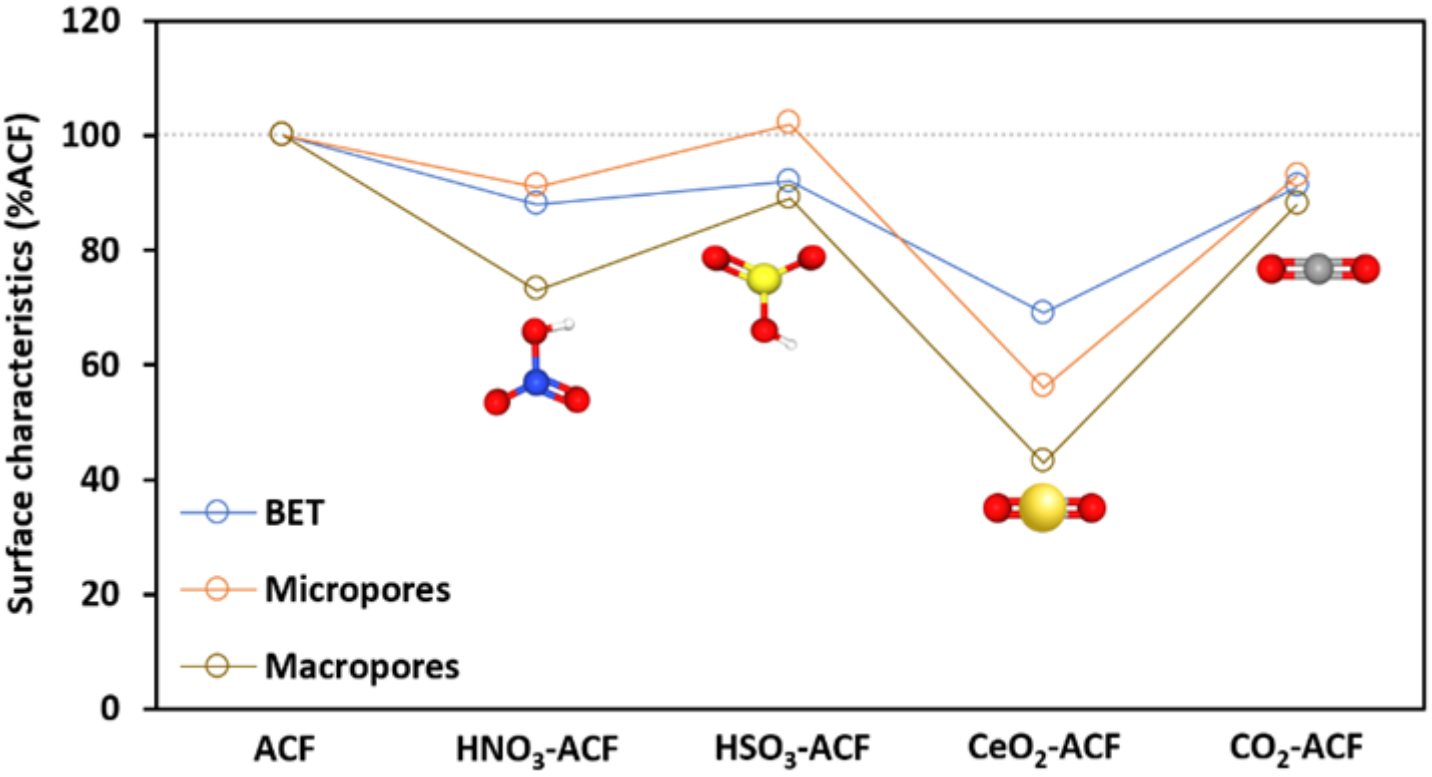

Figure 1

Surface characteristics of carbon fibers via various post-treatments.

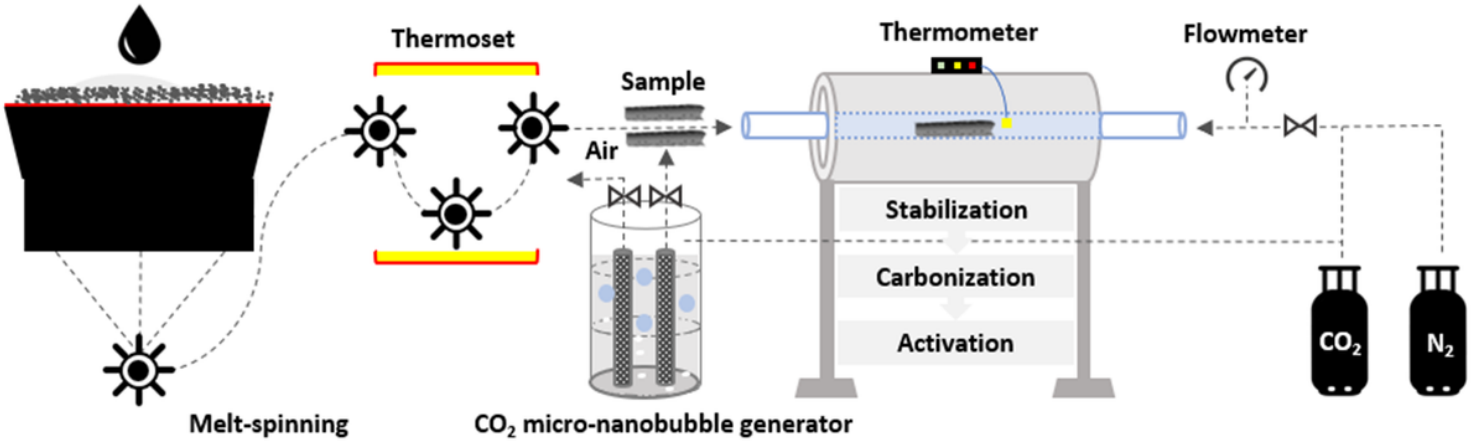

Figure 2

A novel sandwich technique using CO2 in both pretreatment and activation was illustrated. The introduction of micro-bubbles via CO2 micro-nanobubble generator before stabilization was first proposed. Normal size of CO2 gas was subsequently injected during activation for 3 hr and 6 hr, respectively.

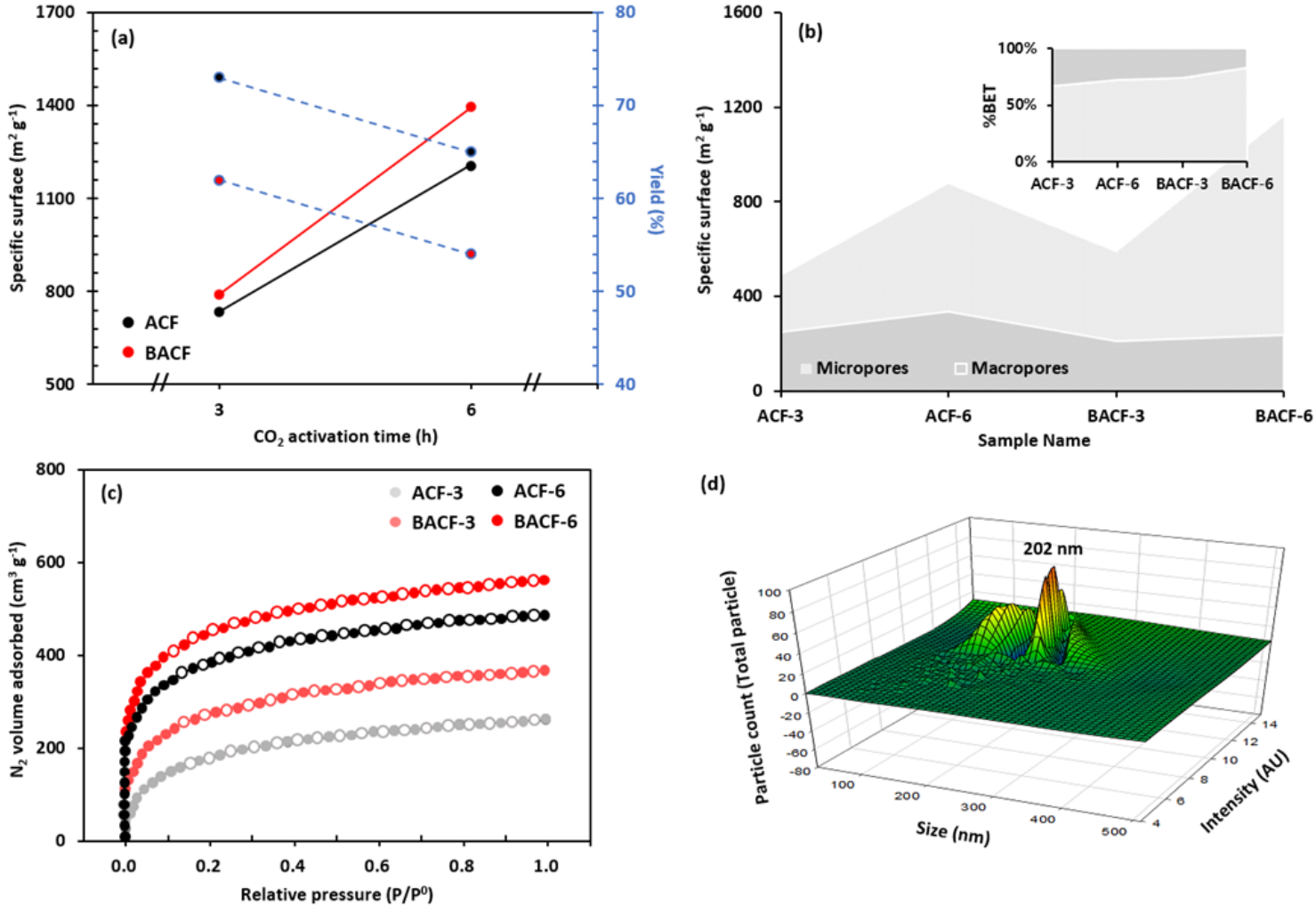

Figure 3

Surface characteristics of (a) BET specific surface (left black-colored) and the final yield of samples after activation (right blue-colored). Micropores and macropores are plotted in (b), whereas the inert graph shows the proportion of the aforementioned in the view of the total BET specific surface. N2 volume adsorption-desorption isotherms are listed in (c). With the aid of the nanoparticle tracking method, median size of 202 nm was observed as can be seen in (d). The concentration was 2.31 × 1010 particle ml−1. Within the figure, ACF and BACF refer to activated carbon fibers and micro-nanobubble-treated activated carbon fibers. Numbers after the sample name is the activation time.

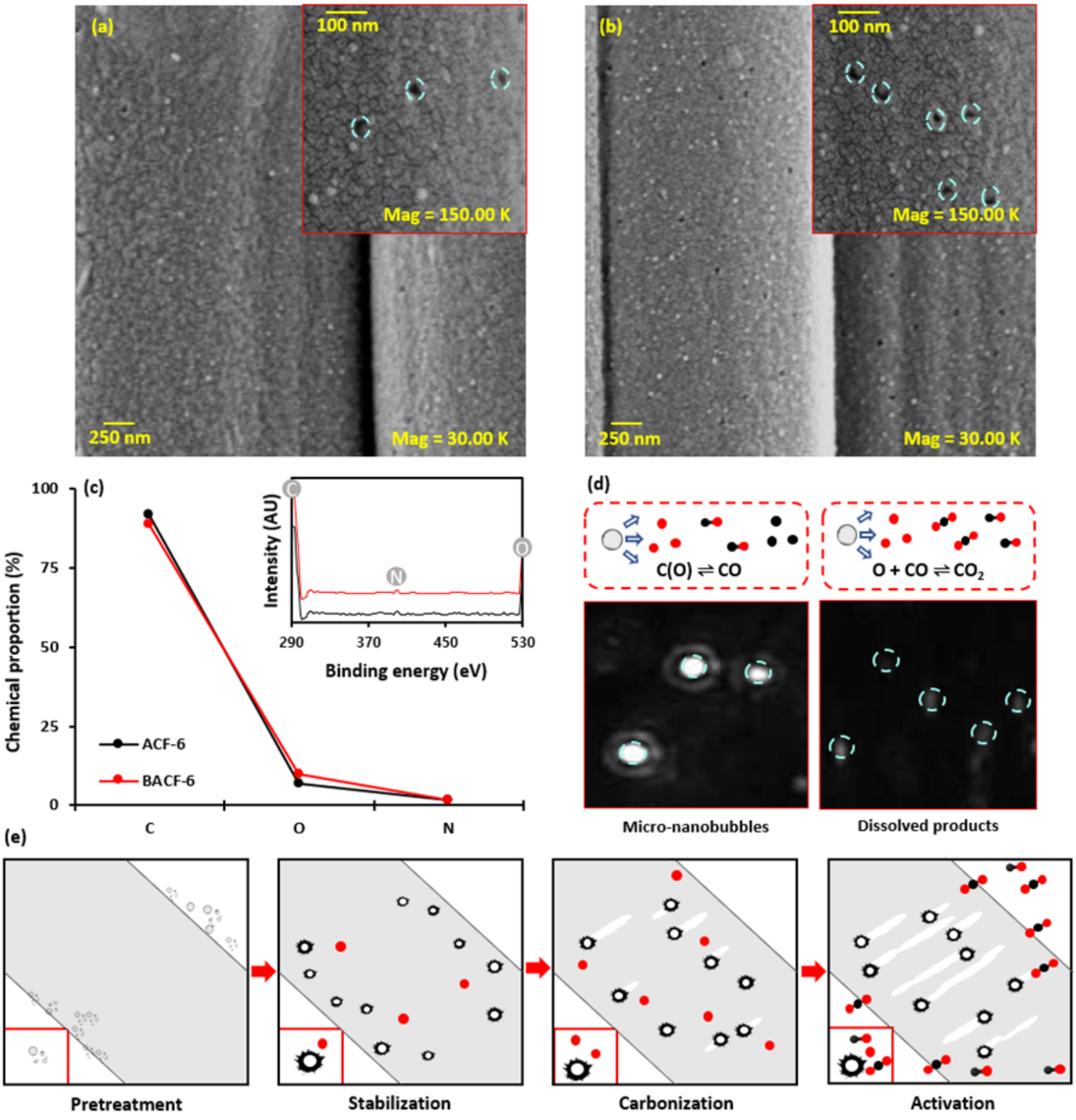

Figure 4

SEM images of (a) ACF-6 and (b) BACF-6 at two different magnification; 30.00 K and 150.00 K (inert). Pore characteristics are more visible on the right side of carbon fibers compared to the left side. The average chemical proportion via EDX and XPS is plotted in (c). Possible impurities between C1s and O1s peaks were further examined (inert). The proposed chemical equations using micro-nanobubbles as a feedstock are illustrated in (d). Micro-nanobubbles (CO_2) and dissolved products (O) scanned via nanoparticle tracking analysis are shown below. (e) A conceptual sketch of the mechanism underlying the introduction of bullet-like micro-nanobubbles may act as an advance team at the frontline of stabilization. The illustrated micro-nanobubbles in pretreatment and stabilization are drawn as micro-nanoscale, but some macroscale droplets can also coexist. Micro-nanobubbles are colored light grey and surface holes white. C atoms are colored black and O atoms red. Within the figure, ACF and BACF refer to activated carbon fibers and micro-nanobubble-treated activated carbon fibers. Numbers after the sample name is the activation time.

Supplementary Files

This is a list of supplementary files associated with this preprint. Click to download.

- SupplementalMaterial.docx